Kelvin probe force microscopy of semiconductor surface defects

Y. Rosenwaks* and R. Shikler
Department of Electrical Engineering, Faculty of Engineering, Tel Aviv University, Ramat-Aviv, 69978, Israel

Th. Glatzel and S. Sadewasser
Hahn-Meitner Institut, Glienicker Str. 100, 14109 Berlin, Germany
(Received 7 January 2004; revised manuscript received 30 March 2004; published 31 August 2004)

We present a comprehensive three-dimensional analysis of Kelvin probe force microscopy of semiconductors. It is shown that high-resolution electronic defect imaging is strongly affected by free carrier electrostatic screening, and the finite size of the measuring tip. In measurements conducted under ambient conditions, defects that are not more then 2 nanometers below the surface, and are at least 50 nanometers apart can be imaged only if the tip-sample distance is not larger then 10 nanometers. Under ultrahigh vacuum conditions, when the tip-sample distance can be as small as 1 nanometer, it is shown that the tip-induced band bending is only around a few millivolts, and can be neglected for most practical purposes. Our model is compared to ultrahigh vacuum Kelvin probe force microscopy measurements of surface steps on GaP, and it is shown that it can be used to obtain local surface charge densities.

DOI: 10.1103/PhysRevB.70.085320 PACS number(s): 71.55.−i

I. INTRODUCTION

The electrical properties of semiconductor materials are, to a large degree, governed by defects and dopant atoms incorporated during growth and production processes. Unfortunately, direct experimental access to such bulk point defects is very difficult. In recent years, however, scanning tunneling microscopy (STM) has developed into an ideal tool for the investigation of individual bulk defects and dopant atoms in semiconductors. However STM measurements are limited to highly doped (very conductive) semiconductors, and suffer from tip-induced band bending phenomena. The AFM based Kelvin probe force microscopy (KPFM) technique has already been demonstrated as a powerful tool for measuring electrostatic forces and electric potential distribution with nanometer resolution. The technique has been applied to materials science applications such as: work function mapping,[1] and ordering in III-V compound semiconductors.[2] Kikukawa *et al.* have conducted surface potential measurements of silicon *pn* junctions,[3] and Vatel *et al.* have demonstrated potential measurements of resistors,[4] and *n*-*i*-*p*-*i* heterostructures.[5] KPFM has also proved to be effective in electrical characterization of submicron devices like high electron mobility transistors (HEMT's),[6] light emitting diodes[7] and thin film solar cells.[8] In addition, several groups have used the technique for two-dimensional surface dopant profiling,[9] and were able to distinguish relative changes in dopant concentration with lateral resolution of less than 100 nm.

Imaging of charged dopants or other surface or subsurface charged features could be achieved using KPFM; however, it has been proved extremely difficult especially under ambient conditions. Brus *et al.*[10] have reported on measurements of the electrostatic charge and photoionization characteristics of 5 nm CdSe nanocrystals using electrostatic force microscopy in dry air, and Sommerhalter *et al.*[11] have succeeded to obtain high resolution KPFM images of single semiconductor surface steps under ultrahigh vacuum conditions.

In this work we examine the factors affecting the sensitivity and resolution of KPFM for semiconductors measurements both under ambient and ultrahigh vacuum (UHV) conditions. A rigorous analysis of the electrostatic interaction between the measuring AFM tip and the semiconductor surface shows that both electrostatic screening and the tip-averaging effect substantially decrease the KPFM sensitivity and resolution. However, measurements conducted under UHV conditions allow to image atomic size defects, and to obtain their trapped charge concentration. Following a short introduction to KPFM in the next section, Secs. III and IV analyze the effects of screening, and of the measuring tip, and our model is compared to high resolution measurements in Sec. V.

II. BASIC DEFINITIONS

The contact potential difference (CPD) between two materials, for example, between an AFM tip and a sample, is defined as

$$V_{\mathrm{CPD}} = \frac{\phi_{\mathrm{tip}} - \phi_{\mathrm{sample}}}{-q}, \quad (1)$$

where ϕ_{tip} and ϕ_{sample} are the work functions of the tip and the sample, respectively, and q is the elementary charge. Therefore, if an AFM tip and a semiconductor with different work functions are held in close proximity to each other a force will develop between them, due to the potential difference V_{CPD}; this is schematically described in Fig. 1. When the two materials are not connected their local vacuum levels are aligned but there is a difference in their Fermi levels. Upon electrical connection the Fermi levels will align by means of electron current, as shown in Fig. 1(a). The two materials (electrodes) are now charged and there is a difference in their local vacuum levels. Due to the charging of the tip and the sample, an electrostatic force develops as shown

 ©2004 The American Physical Society

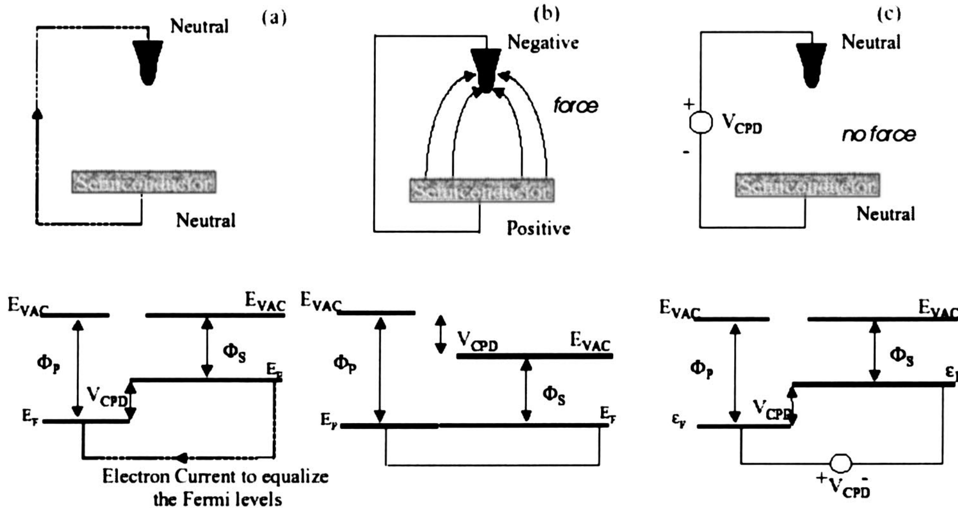

FIG. 1. Definition and basic measurement setup of contact potential difference (CPD).

in Fig. 1(b). This force can be nullified by applying an external bias between the tip and the sample. The magnitude of this bias is the contact potential difference and its sign depends whether it is applied to the sample or to the tip.[12]

A typical KPFM measurement is conducted in the following way. An AC bias at a frequency ω is applied between the tip and the sample. It is shown below[13] that the force component at this frequency is proportional to the CPD and therefore, can be nullified using a feedback loop whose input is the component of the electrostatic force at a frequency of ω. The simplest approximation of this force is to treat the tip-sample system as a parallel plate capacitor with one plate being the tip apex, and the other the sample underneath it.[9] Under this assumption the force which is the derivative of the electrostatic energy with respect to the tip-sample separation, z, is given by

$$F=-\left.\frac{\partial U}{\partial z}\right|_{Q}=-\frac{1}{2}V^2\frac{\partial C}{\partial z}, \tag{2}$$

where the electrostatic energy U is given for a parallel plate capacitor configuration by $U=\frac{1}{2}CV^2$ with C the tip-sample capacitance, and V the potential difference between the two capacitor plates. Using the following expression for the potential difference: $V=V_{\mathrm{dc}}-V_{\mathrm{CPD}}+V_{\mathrm{ac}}\sin(\omega t)$ where V_{DC} is a nullifying voltage applied in order to measure the CPD and inserting it in Eq. (2) gives for the force at a frequency ω,

$$F_\omega=\frac{1}{2}\frac{\partial C}{\partial Z}(V_{\mathrm{CPD}}-V_{\mathrm{DC}})V_{\mathrm{ac}}\sin(\omega t). \tag{3}$$

Equation (3) although used by many authors is strictly correct only for a metallic sample and when the tip-sample system can be approximated as a parallel plate capacitor configuration. Hudlet *et al.*[13] have presented a detailed one-dimensional analysis of the electrostatic force between a tip and a semiconductor, and have shown that the force at a frequency of ω can be expressed as

$$F_\omega=\frac{Q_{ss}}{\varepsilon_0}C_{\mathrm{eff}}V_{\mathrm{ac}}\sin(\omega t), \tag{4}$$

where Q_{ss} is the semiconductor surface charge, ε_0 is the dielectric constant, and C_{eff} is the effective capacitance of the electrode-air/vacuum-semiconductor system. For a metallic sample where Q_{ss} is replaced by $C(V_{\mathrm{CPD}}-V_{\mathrm{DC}})$, and C_{eff} by C (where C is the tip-metallic sample capacitance), Eq. (4) reduces to Eq. (3).

III. ELECTROSTATIC SCREENING IN SEMICONDUCTORS

Electrostatic screening is a well-known phenomenon in which charges of one type rearrange themselves around charges of the opposite type in order to minimize the total electrostatic energy. Thus if we want to measure a charged defect using KPFM, the screening by the free carriers will reduce the local surface band bending resulting from the defect. The local surface potential resulting from a charged defect located at different distances from the semiconductor surface, i.e., the defect screening length, was calculated as follows. A silicon sample with a doping of 10^{17} cm^{-3} and an average band bending of 0.12 eV was used for the calculations. The following Poisson equation:

$$\nabla^2 V=\frac{q}{\varepsilon}\left(n_i\left(\exp\left(\frac{V}{V_T}\right)-\exp\left(-\frac{V}{V_T}\right)\right)-D\right), \tag{5}$$

was solved. Where ε is the semiconductor dielectric constant, D is the net dopant concentration, and V_T is the thermal voltage defined as $V_T\equiv kT/q$. At the semiconductor-air/vacuum interface, the following boundary condition:

$$\varepsilon E_{\mathrm{semi}}-\varepsilon_0 E_{\mathrm{air/vac}}=Q_{ss}=-\frac{n_{ss}}{1+\exp\left(\frac{E_{ss}-E_F}{kT}\right)}, \tag{6}$$

was used. Where E_{semi} and $E_{\mathrm{air/vac}}$ are the electric fields on both sides of the semiconductor-air/vacuum interface, ε_0 is the air/vacuum permittivity, n_{ss} is the density of surface states, and E_{ss} is their energy assuming acceptor like surface

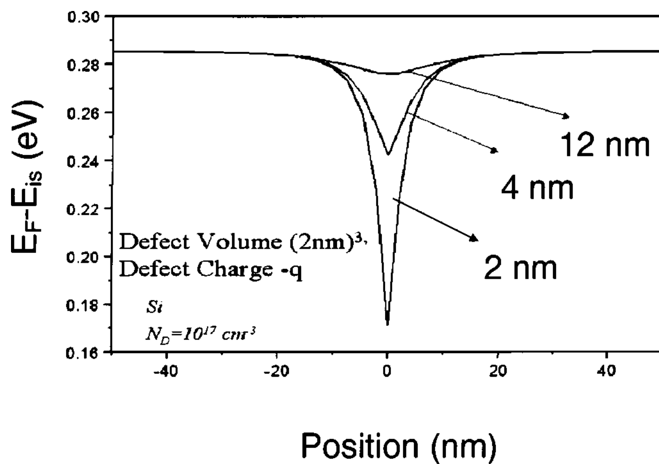

FIG. 2. Calculated local band bending, expressed as $(E_F - E_{is})$ for Si having a background average band bending of 0.12 volt. The calculation is conducted for a charged defect (total charge q) located at three different distances (2, 4, and 12 nm) from the crystal surface.

states.[14] For all the other boundaries we have used the Neumann boundary conditions, i.e., $\nabla_n V = 0$ where ∇_n is the derivative normal to the surface. The equations were discretisized using a finite difference model[15] and then solved using the fixed point iteration method combined with successive over relaxation.[16] In this method, the difference equations resulting from the discretization process are solved at each grid point. When these equations are nonlinear, a single step Newton-Raphson scheme is used, while for the linear case a simple successive over relaxation method is applied.

Figure 2 shows the local band bending (surface potential) calculated using the method described above for defects located at three different distances (of 2, 4, and 12 nm) below the semiconductor surface. The figure shows that when a charged defect is located 2 nm below the surface the local change in the surface band bending is ~100 mV; however if the defect is positioned 12 nm below the surface, the local band bending at the surface is only around 5 mV which is the typical sensitivity of the KPFM measurements.[7] This implies that the KPFM method is sensitive to defects which are not more than a few nanometers below the semiconductor surface. Even then, the average equivalent defect density must be larger than $1/(2\times10^{-7})^3 \sim 1\times10^{20}$ cm^{-3} so that the surface band bending will be larger than a few mV in order to be measurable.

IV. THE EFFECT OF THE MEASURING TIP

A. Tip size and geometry

It is well known that the finite tip size in scanning probe microscopies has a profound effect on the measured image. In electrostatic force based microscopies the effect of the measuring tip is much larger because the measured forces have an infinite range. Tip effects in electrostatic force and Kelvin probe microscopies were discussed and analyzed by several authors. One of the simplest models was suggested by Hochwitz *et al.*[17] who modeled the tip by a series of (staircase) parallel plate capacitors. Hudlet *et al.*[18] have presented an analytical evaluation of the electrostatic force between a conductive tip and a metallic surface, while Belaidi *et al.*[19] have calculated the forces and estimated the resolution in a similar system. Jacobs *et al.*[20] have extended the calculations for the case of a semiconductor sample, by replacing its surface by a set of ideal conductors with mutual capacitances between them. All the above analyses and many others show that even for a very small tip-sample distance of 5 nm the lateral resolution and the measured KPFM signal are largely affected by the tip-averaging effect.

To the best of our knowledge almost all the papers that analyze semiconductor KPFM measurements replace the semiconductor sample by a surface with a fixed or variable potential. This is only valid for the case of a weakly interacting tip-sample system, i.e., when there is no tip-induced band-bending phenomenon. As described above a typical KPFM measurement is conducted by nullifying the electrostatic force at a frequency of ω, using an external bias-V_{DC}. Thus a calculation of the KPFM signal amounts to finding the voltage applied to the tip or to the sample,[13] V_{DC}, that minimizes the total electrostatic force at the frequency ω. Below we calculate the static (DC) electrostatic force; i.e., it is assumed that the AC voltage has a negligible effect on the tip-sample forces. This is justified based on the fact that the frequency ω used in the measurements (>300 kHz) is high and in addition the AC modulation amplitude applied to the tip is very low (100 mV).[21]

The electrostatic force was calculated as follows. First the electric field, E, for the semiconductor-air/vacuum-tip system is calculated using Eq. (5); assuming that the tip is a perfect conductor, the electrostatic force is then calculated by integrating the Maxwell stress over the entire tip surface,

$$F = -\left.\frac{dU}{dz}\right|_{Q=\text{const}} = -\frac{1}{2\varepsilon_s}\oint_S |E|^2 d\hat{S}\cdot\hat{z}, \qquad (7)$$

where U is the electrostatic energy of the system, $d\hat{S}$ is a tip surface element, and $\hat{z}$ is a unit vector in the z (perpendicular to the semiconductor surface) direction.

Figure 3 shows the CPD (calculated using the method described above) between a tip located at different heights above the same Si sample used for the calculations presented in Fig. 2; here all the calculations were carried out for a defect (total charge q) located 2 nm below the surface. The figure shows the large tip averaging effect when a small single defect is to be imaged. When the tip is in at 0 [no electrical contact, curve (d)] or 1 nm above the surface [curve (c)], the calculated CPD is almost identical with the band bending calculation represented by the bottom curve in Fig. 2; in other words, the CPD that will be measured in such a case will be unchanged by the measuring tip and thus corresponds to the real band bending. However, when the tip is 5 nanometers above the surface, the CPD magnitude decreases by a factor of 3 (from 100 to 30 mV), and when the tip height increases to 30 nm the local potential change is only around 5 mV. This implies that in ambient KPFM measurements (where a typical tip-surface distance is

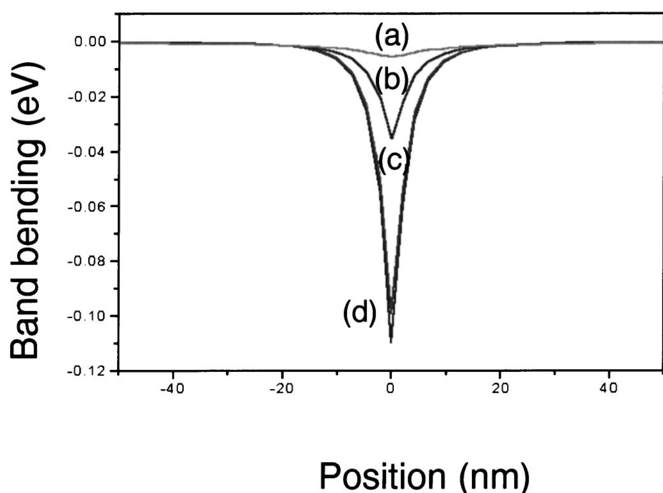

FIG. 3. Calculated local band bending, expressed as $(E_F - E_{is})$ for Si having a charged defect (total charge q) located at a distance of 2 nm below the crystal surface. The calculation is conducted for four different tip-sample distances of zero [no electrical contact (d)], 1 (c), 5 (b), and 30 (a) nanometers. The figure demonstrates that under ambient conditions (typical tip-sample distance of ~30 nm) single electronic defects cannot be imaged.

20–30 nanometers due to the amplitude of the vibrating tip required to obtain a reasonable signal-to-noise ratio) small defect imaging would be impossible. This explains why KPFM images of semiconductor surfaces are typically featureless, with no evidence for charged surface states.

A similar approach for electrostatic force calculations was applied in the past for a metallic sample where the sample surface potential was assumed constant.[19] However, here we calculate whether the presence of the tip has any significant effect on the semiconductor surface potential, i.e., is there any tip-induced band bending at the semiconductor surface. Thus, our calculation takes into account the electrostatic energy present when the semiconductor energy bands are not flat due to the presence of surface states and/or due to tip-induced band bending. Hudlet *et al.*[13] have shown that in the one-dimensional case, the tip-sample system can be modeled as two capacitors in series. Thus, when the distance between the sample and the tip is reduced, the sample capacitance cannot be neglected and it changes the force acting on the tip, and the measured CPD.

We have calculated the surface induced band bending for a tip, having a potential of 0.1 volt higher then the sample surface ($n = 5 \times 10^{17}$ cm^{-3} GaP with no charged surface states, or zero band bending) and located 5 nm above it; the result is shown in Fig. 4. The figure shows that the surface band bending, expressed as $(E_F - E_{is})$ where E_{is} is the surface Fermi level position, due to the presence of the biased tip, is zero everywhere except for a small region in the middle where the band bending is less than 6 mV. A similar calculation conducted for a tip-sample surface potential difference of 0.6 volt resulted in an induced surface band bending of around 38 mV.[22]

The small-induced band-bending effect can be explained in the following way. The tip-vacuum-semiconductor system can be modeled as two capacitors, tip-vacuum-semiconductor surface and the semiconductor space charge region (SCR) connected in the series. Thus an external voltage (in the present case it is the semiconductor-tip CPD) will drop mainly on the smaller of the two capacitors. The SCR capacitance is typically much larger (except for very low doped semiconductors) thus causing the voltage to drop mainly between the tip and the sample surface, and hence inducing a negligible band bending in the SCR. It must be re-emphasized that in KPFM measurements the CPD between the tip and the sample is nullified, so typically the potential difference between any point on the tip, and on the sample surface in a close distance to it, will be even lower then the 0.1 V used in calculating the potential in Fig. 4. In summary, the dominant contribution to the tip-sample electrostatic force is from the tip-vacuum-sample surface capacitor and the SCR capacitance can be neglected in most cases. Thus, such an assumption used by Hochwitz *et al.*,[17] Hudlet *et al.*,[18] and Jacobs *et al.*[20] is correct. Furthermore, the above conclusion simplifies tremendously the simulation of semiconductors KPFM measurements. This is because it requires solving only the Laplace equation using fixed (potential independent) boundary conditions at the semiconductor surface.

V. COMPARISON WITH EXPERIMENTAL RESULTS

Our model is compared with measurements conducted at GaP (110) surface steps using UHV-KPFM. The KPFM setup is a modified UHV-AFM (Omicron Inc.) operated at

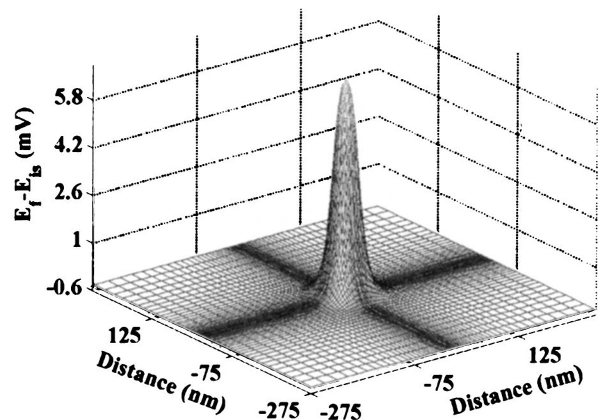

FIG. 4. Calculated local band bending, expressed as $(E_F - E_{is})$ for a GaP with no surface states, tip-sample distance of 5 nm, and an applied bias of $V_{tip} = 0.1$ V between tip and sample. The protrusion in the center is the tip-induced band bending at the GaP surface.

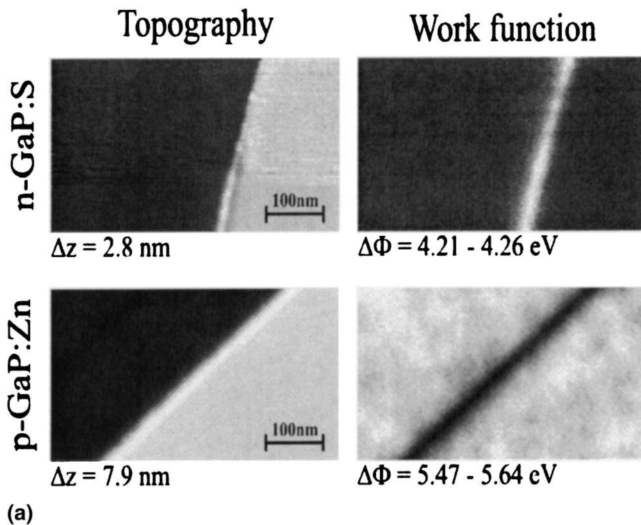

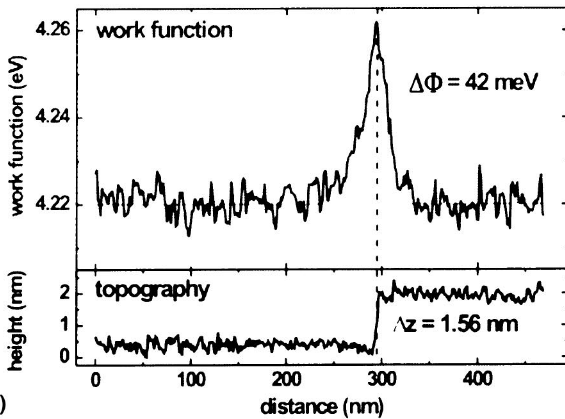

FIG. 5. (a) Topography (left) and work function (right) measured by UHV-KPFM on cleaved n-GaP (top) and p-GaP (bottom) (110) surfaces; for the n-GaP the step runs along the [111] direction, whereas in the p-GaP the step runs along the [211] direction. (b) Line scans showing the CPD increase (top) and the topography change for the n-GaP sample.

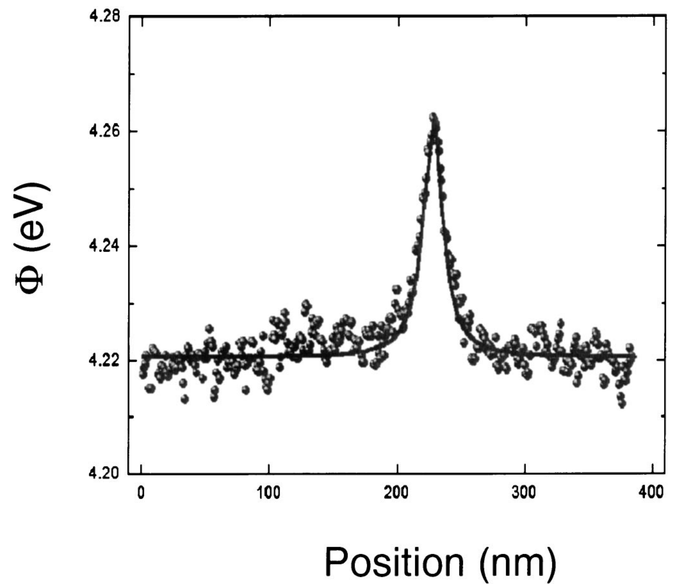

FIG. 6. Calculated CPD (solid line) together with the KPFM measurement (dotted line) of the step on the cleaved n-GaP (110) surface. The CPD was calculated for a tip height of 5 nm, and charge densities of $n_{ss}^{(110)}=(6\pm2)\times10^{11}$ cm^{-2} and $n_{ss}^{\text{step}}=(1.2\pm0.2)\times10^{6}$ cm^{-1}, respectively.

$p\leqslant10^{-10}$ mbar that was described in detail in the past.[11] The topography is measured using the conventional frequency modulation technique at the first cantilever resonance frequency (~75 kHz); the AC voltage (100 mV in amplitude) for the detection of the contact potential difference (CPD) is tuned to the second resonance frequency of the cantilever. This allows a highly sensitive, simultaneous and independent detection of the electrostatic forces with a sensitivity of ~5 meV and tip-sample distance of ~5 nm. S-doped ($n\approx5\times10^{17}$ cm^{-3}) and Zn-doped ($p\approx5\times10^{18}$ cm^{-3}) well-defined GaP (110) surfaces were obtained by cleavage inside the UHV chamber.

Figure 5(a) shows the topography (left) and the work function (right) of the UHV-KPFM measurement on the n-(top) and p-doped (bottom) GaP (110) surface; additionally, representative topography and CPD line profiles for the n-GaP are plotted in (b). It is clearly seen that the work function changes are associated with the step, exhibiting a work function increase along the step edge. The work function for the (110) surface (excluding the steps) was found to be $\Phi=4.22$ eV, and 5.61 eV for the n and p type, respectively. The work function change at the step edge is $\Delta\Phi_{\text{step}}=42$ and 135 meV for the n- and p-type samples, respectively. The corresponding topography variations are 1.6 and 6.4 nm, respectively. The work function change ($\Delta\Phi_{\text{step}}$) on the p-GaP surface is larger because the height of the specific step is much larger. The observation that the CPD increases (decreases) at the steps on the n (p) surfaces, excludes a topography induced artifact and supports our hypothesis (discussed in detail below) that these changes are due to local band bending induced by charged surface gap states located at the steps.

Figure 6 shows a calculation of the CPD (solid line) compared with the UHV-KPFM measurement (dots) of the atomic step on the cleaved n-GaP (110) surface. The fitting was carried out in the following way. First we have calculated the CPD resulting from a Gaussian potential distribution 0.1 V high and 50 nm (standard deviation) wide. The results are shown in Fig. 7 for four different tip-sample distances. The figure shows that for a tip height of 5 nm, the calculated CPD profile is reduced by a factor of around 2.5, and its width is increased by a factor of 2 relative to the theoretical surface potential represented by the top curve. The surface charge density at the step was extracted by fitting the measured CPD to the calculated surface potential, assuming that the surface states induced by the steps are only at the sample surface.

These assumptions reduce the number of unknown (fitting) parameters to two: the charge density at the atomic step, and that of the (110) surface. The calculation is preceded by assuming two initial values for these two surface charge densities, and then the 3D semiconductor surface potential distribution is calculated using Eq. (5). We then cal-

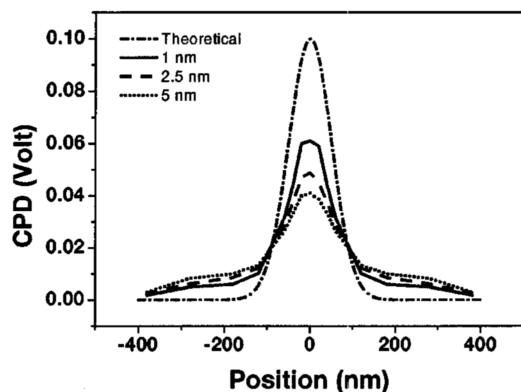

FIG. 7. Calculated CPD for a Gaussian surface potential distribution at four different tip heights above the semiconductor surface.

culate the measured CPD in the presence of the tip and compare the result with the measurement; this procedure is repeated, by changing both the (110) surface charge, and the charge at the step until a good visual fit like the one shown in Fig. 6 is obtained. This fit was obtained using (110) and step charge densities of $n_{ss}^{(110)}=(6\pm2)\times10^{11}$ cm^{-2} and $n_{ss}^{\mathrm{step}}=(1.2\pm0.2)\times10^{6}$ cm^{-1}, respectively. The surface charge is an areal density, whereas the step charge is a line density.

A similar quality fit could not be achieved using different combinations of the two charge densities; this is because the width of the Gaussian CPD profile at the step is much more sensitive to the surrounding charge density (screening effect), while its magnitude strongly depends on the charge density at the step. Moreover, these results are in good agreement with measured work functions of the surrounding areas in both samples; this is explained as follows. A surface charge density of $n_{ss}^{(110)}=(6\pm2)\times10^{11}$ cm^{-2} corresponds to depletion type band bending of $\cong$0.4 eV on both the p and n sides. Such band bending will increase (decrease) the work function of the n (p) surfaces by a total of 0.8 eV, thus reducing the work function difference between the n and p sides to $2.1-0.8=1.3$ eV; 2.1 eV is the work function difference calculated for the present n- and p-doping concentrations. This is in agreement with the measured work function difference of $5.61-4.22=1.39$ eV between the p- and n-type material [see Fig. 1(a)].

The error in the charged surface states density at the step calculated using a semiclassical (versus quantum mechanical) approach is small based on the following reason. The average distance between the charged states at the step can be estimated (based on the surface line charge from the fit of Fig. 5) as $\sim1/(1.2\times10^{6}\text{ cm}^{-1})=83$ Å. On the other hand, it is known[23] that the extension of the wave functions of electrons localized in deep sub-band-gap states is smaller by about one order of magnitude. In addition, the trapped charge at the step can be approximated as a line of noninteracting point charges in a similar way to that described by Heinrich *et al.*[24] A simple calculation of the potential of such a charge distribution gives a potential in the range of 0.1 volt, which is in agreement with our KPFM measurement. If we assume that the charge measured at the step is largely due to sub-band-gap surface states induced by dangling bonds (due to Ga or P terminated step edges), our results correspond to trapped charge density of about 1e per $\sim$50 lattice spacings [assuming that the measured step height in Fig. 1(a) is $\sim$3 lattice spacings]. It is very likely that the step reconstructs following the cleavage such that only around 2% $(1/50)$ out of the dangling bonds remain unconstructed, charged, and induce the sub-band-gap charged states.

VI. SUMMARY AND CONCLUSIONS

We have presented a comprehensive three-dimensional analysis of Kelvin probe force microscopy of semiconductors. It was shown that electrical defects imaging is strongly affected by both the free carrier electrostatic screening and the finite size of the measuring tip. In measurements conducted under ambient conditions, defects which are not more than 2 nanometers below the surface, have an equivalent charge density of $>10^{20}$q cm^{-3}, and are at least 50 nanometers apart can be measured only if the tip-sample distance is not larger than 10 nanometers. Under ultrahigh vacuum conditions, when the tip-sample distance can be as small as 1 nanometer, the tip-induced band bending is less than a few millivolts, and can be neglected for most practical purposes. The model is compared to ultrahigh vacuum Kelvin probe force microscopy measurements of surface steps on GaP, where it is shown that it can be used to obtain local surface charge densities.

ACKNOWLEDGMENTS

This research was conducted within the 5th European research network Herculas, and the authors acknowledge fruitful discussions with Professor M. Molotskii.

*Corresponding author. Email address: yossir@eng.tau.ac.il

[1] M. Nonenmacher, M. P. O'Boyle, and H. K. Wickramasing, Appl. Phys. Lett. **58**, 2091 (1991).
[2] Y. Leng, C. C. Williams, L. C. Su, and G. B. Stringfellow, Appl. Phys. Lett. **66**, 1264 (1995).
[3] A. Kikukawa, S. Hosaka, and R. Imura, Appl. Phys. Lett. **66**, 3510 (1995).
[4] O. Vatel and M. Tanimoto, Appl. Phys. Lett. **77**, 2358 (1995).
[5] A. Chavez-Pirson, O. Vatel, M. Tanimoto, H. Ando, H. Iwamura, and H. Kanbe, Appl. Phys. Lett. **67**, 3069 (1995).
[6] T. Mizutani, M. Arakawa, and S. Kishimoto, IEEE Electron Device Lett. **18**, 423 (1997); M. Arakawa, S. Kishimoto, and T. Mizutani, Jpn. J. Appl. Phys., Part 1 **36**, 1826 (1997).
[7] R. Shikler, N. Fried, T. Meoded, and Y. Rosenwaks, Appl. Phys. Lett. **74**, 2972 (1999); R. Shikler, T. Meoded, N. Fried, B. Mishori, and Y. Rosenwaks, J. Appl. Phys. **86**, 107 (1999).
[8] S. Sadewasser, Th. Glatzel, M. Rusu, A. Jäger-Waldau, and M. Ch. Lux-Steiner, Appl. Phys. Lett. **80**, 2979 (2002); Th. Glatzel,

D. Fuertes Marrón, Th. Schedel-Niedrig, S. Sadewasser, and M. Ch. Lux-Steiner, *ibid.* **81**, 2017 (2002).
[9] A. K. Henning, T. Hochwitz, J. Slinkman, J. Never, S. Hoffman, P. Kaszuba, and C. Daghlian, J. Appl. Phys. **77**, 1888 (1995).
[10] T. D. Krauss, S. O'Brien, and L. E. Brus, J. Phys. Chem. B **105**, 1725 (2001).
[11] Ch. Sommerhalter, Th. W. Matthes, Th. Glatzel, A. Jäger-Waldau, and M. Ch. Lux-Steiner, Appl. Phys. Lett. **75**, 286 (1999).
[12] The sign of the measured V_{CPD} will be positive (negative) if the nullifying voltage is applied to the sample (tip), respectively, see Ref. 7.
[13] S. Hudlet, M. S. Jean, B. Roulet, J. Berger, and C. Guthmann, J. Appl. Phys. **59**, 3308 (1995).
[14] The energy of the acceptorlike surface states (E_{ss}) is not of an importance here, and the energy level was chosen such that the charge density obtained from the fit is not sensitive to it. The emphasis is on calculating the total surface charge density, as their energy distribution cannot be determined at this stage.
[15] I. D. Mayergoyz, J. Appl. Phys. **59**, 195 (1986).
[16] C. E. Korman and I. D. Mayergoyz, J. Appl. Phys. **68**, 1324 (1990).
[17] T. Hochowitz, A. K. Henning, C. Levey, C. Daghlian, and J. Slinkman, J. Vac. Sci. Technol. B **14**, 457 (1996).
[18] S. Hudlet, M. Saint Jean, C. Guthmann, and J. Berger, Eur. Phys. J. B **2**, 5 (1998).
[19] S. Belaidi, F. Lebon, P. Girard, G. Leveque, and S. Pagano, Appl. Phys. A: Mater. Sci. Process. **66**, S239 (1998).
[20] H. O. Jacobs, H. F. Knapps, S. Muller, and A. Stemmer, J. Appl. Phys. (to be published).
[21] We have studied extensively the effect of the AC modulation amplitude and frequency in the past; it was found (see Ref. 7) that even for much larger V_{AC} amplitudes and at lower frequencies, the measured CPD is unchanged.
[22] R. Shikler, Ph.D. thesis, Tel-Aviv University, 2003.
[23] The theory of zero radius potential, see for example, E. Pantelidis, Rev. Mod. Phys. **50**, 797 (1978).
[24] M. Heinrich, C. Domke, Ph. Ebert, and K. Urban, Phys. Rev. B **53**, 10 894 (1996).